

# Dielectric anomaly and magnetic response of epitaxial orthorhombic YMnO<sub>3</sub> thin films

X. Martí<sup>a)</sup>

*Institut de Ciència de Materials de Barcelona, Consejo Superior de Investigaciones Científicas (CSIC), Campus UAB, Bellaterra 08193, Spain*

V. Skumryev

*Institut Català de Recerca i Estudis Avançats (ICREA), Barcelona, Spain; and Departament de Física, Universitat Autònoma de Barcelona, Bellaterra 08193, Spain*

V. Laukhin

*Institut de Ciència de Materials de Barcelona, Consejo Superior de Investigaciones Científicas (CSIC), Campus UAB, Bellaterra 08193, Spain; and Institut Català de Recerca i Estudis Avançats (ICREA), Barcelona, Spain*

F. Sánchez

*Institut de Ciència de Materials de Barcelona, Consejo Superior de Investigaciones Científicas (CSIC), Campus UAB, Bellaterra 08193, Spain*

M.V. García-Cuenca, C. Ferrater, and M. Varela

*Departament de Física Aplicada I Òptica, Universitat de Barcelona, Diagonal 647, Barcelona 08028, Spain*

J. Fontcuberta

*Institut de Ciència de Materials de Barcelona Consejo Superior de Investigaciones Científicas (CSIC), Campus UAB, Bellaterra 08193, Spain*

(Received 26 December 2006; accepted 21 March 2007)

The structure, magnetic response, and dielectric response of the grown epitaxial thin films of the orthorhombic phase of YMnO<sub>3</sub> oxide on Nb:SrTiO<sub>3</sub> (001) substrates have been measured. We have found that a substrate-induced strain produces an in-plane compression of the YMnO<sub>3</sub> unit cell. The magnetization versus temperature curves display a significant zero-field cooling (ZFC)-field cooling hysteresis below the Néel temperature ( $T_N \approx 45$  K). The dielectric constant increases gradually (up to 26%) below the  $T_N$  and mimics the ZFC magnetization curve. We argue that these effects could be a manifestation of magnetoelectric coupling in YMnO<sub>3</sub> thin films and that the magnetic structure of YMnO<sub>3</sub> can be controlled by substrate selection and/or growth conditions.

## I. INTRODUCTION

Understanding and tailoring coupling between the magnetic and dielectric properties of oxides is a very active field of research. The ultimate goal, to control the magnetic (dielectric) state by using an electric (magnetic) field, requires that both physical properties are coupled. Manganese oxides AMnO<sub>3</sub>, where A is a suitable rare earth, present a hexagonal or perovskite (orthorhombic) structure, depending on the size of the rare-earth cation; for the smaller rare earths (Ho–Lu, Y), the hexagonal phase (in bulk) is the equilibrium phase, whereas the orthorhombic phase is obtained for the larger rare earth (Tb, Dy, and Gd). Of relevance here is that, whereas at low temperature both families of compounds display an antiferromagnetic (AF) order, the ferroelectric (FE) order sets in at temperatures [i.e., FE Curie temperature ( $T_C^{FE}$ )]

much above the AF Néel temperature ( $T_N$ ) in the hexagonal structure, but it occurs at temperatures below the  $T_N$  in materials with orthorhombic structures. For instance: for the hexagonal YMnO<sub>3</sub>,  $T_C^{FE}$  is  $\sim 900$  K and  $T_N$  is  $\sim 80$  K,<sup>1,2</sup> and for the orthorhombic TbMnO<sub>3</sub>,  $T_C^{FE}$  is  $\sim 30$  K and  $T_N$  is  $\sim 40$  K.<sup>3</sup>

The magnetism and ferroelectricity usually exclude each other, and thus the occurrence of biferroicity in these oxides has been disputed. Even more intriguing is the existence of some coupling between these ferroic orders. It appears that FE in hexagonal manganites is associated with tilting of the Mn–O octahedral structure,<sup>4</sup> whereas in the orthorhombic TbMnO<sub>3</sub> it has been proposed that FE may result from the existence of a magnetic transition below the  $T_N$  (from sinusoidal to helical spin order) that breaks the spatial inversion symmetry, thus allowing the existence of ferroelectricity.<sup>5</sup>

YMnO<sub>3</sub> is on the verge of stability between hexagonal and orthorhombic phases. Although under normal synthesis conditions, the hexagonal phase is the stable one,

<sup>a)</sup>Address all correspondence to this author.

e-mail: fontcuberta@icmab.es

DOI: 10.1557/JMR.2007.0264

the metastable orthorhombic o-YMnO<sub>3</sub> phase can be obtained using either high pressures (bulk materials)<sup>6</sup> or appropriate epitaxial strain engineering (thin films).<sup>7–9</sup> It has been reported that polycrystalline o-YMnO<sub>3</sub> displays a pronounced dielectric constant ( $\epsilon$ ) anomaly at  $T\epsilon < T_N$ ,<sup>10</sup> which has been taken as a signature of magnetoelectric coupling. The magnetic structure of o-YMnO<sub>3</sub> has been studied in great detail.<sup>11–13</sup> Muñoz et al.<sup>12</sup> concluded that the Mn<sup>3+</sup> spins form a sinusoidally modulated structure (characterized by fluctuating average magnetic moments) defined by a  $(0, C_y, 0)$  mode with the magnetic moments oriented parallel to the propagation vector  $k = (0, k_y, 0)$ . The structure was found to remain stable and incommensurate down to 1.7 K and the propagation vector to be blocked at a constant value below about 28 K.

The existence of a sinusoidal magnetic structure suggests the occurrence of a subtle equilibrium among different magnetic interactions, which are of the superexchange type and thus should be strongly dependent on the Mn–O–Mn bond topology (angles and distances). Therefore, one could expect that epitaxial strain in o-YMnO<sub>3</sub> thin films may affect severely the nature of the magnetic ordering, thus allowing the tuning of the magnetoelectric response.

In this article, we shall address some of these issues. We report first on the stabilization and detailed structural analysis of the epitaxial o-YMnO<sub>3</sub> films on a suitable substrate. Next, we shall provide magnetic and dielectric measurements of these films, and we will show that, for the first time in thin films and in good agreement with earlier reports for polycrystalline materials, the films are magnetically ordered below  $T_N \approx 45$  K and display a well-defined anomaly in  $\epsilon(T)$  at  $T < T_N$ . Interestingly enough, the magnetic data show some irreversibility that indicates the presence of a ferromagnetic component. These results suggest that, indeed, substrate-induced strain can be used to modify the magnetic structure and eventually the dielectric response.

## II. EXPERIMENTAL

YMnO<sub>3</sub> (YMO) thin films were deposited on (001)-oriented 0.5%-Nb:SrTiO<sub>3</sub> (NbSTO) substrates (0.5 mm thick) by pulsed-laser deposition. A KrF excimer laser (wavelength 248 nm; pulse duration 34 ns) was used at a repetition rate of 5 Hz. The laser beam was focused to a fluence of 1.4 J/cm<sup>2</sup> on a stoichiometric YMnO<sub>3</sub> target, with the substrate placed at a distance of 5 cm. The films were deposited at a substrate temperature of 800 °C at an oxygen pressure of 0.2 mbar. At the end of the growth, the samples were cooled down; at 530 °C, 1 atm of oxygen was introduced into the chamber. The growth rate is  $\sim 0.10$  Å/pulse; the thickness of the films was determined from low angle x-ray reflectometry measurements using

Cu K $\alpha$  radiation. The YMO film analyzed here is 150 nm thick. The crystal structure, epitaxial relationships, and lattice strain (out-of-plane and in-plane) were investigated by a Gadds-8 X-ray Bruker diffractometer (Madison, WI).  $\theta$ - $2\theta$  and  $\omega$  scans of symmetrical reflections as well as  $\phi$  scans and pole figures of asymmetrical reflections were measured. Magnetic properties were measured using a superconducting quantum interference device. Dielectric properties were measured, inside a physical property measuring system (PPMS; Quantum Design, San Diego, CA) by using a 16047A Hewlett-Packard (Palo Alto, CA) impedance analyzer. The electrical contacts on the YMO–NbSTO sample with area of 8 mm<sup>2</sup> were made (top and bottom) by using graphite paste. The background impedance of the wiring and substrate was determined by measuring, under nominally identical conditions, the impedance of a bare NbSTO substrate of the same dimensions.

## III. RESULTS AND DISCUSSION

X-ray diffraction experiments have confirmed that the YMO film grown on the Nb:STO(001) substrate is orthorhombic. The  $\theta$ - $2\theta$  scan (Fig. 1) shows the substrate reflections and the (002) and the (004) peaks corresponding to the orthorhombic phase of YMO. There are no traces of either other reflections of the orthorhombic phase or of the hexagonal phase. Thus, within the experimental resolution, the film is purely orthorhombic, and it is (001) textured; we used the *Pbnm* setting ( $a = 5.26$  Å,  $b = 5.85$  Å,  $c = 7.36$  Å in bulk YMO). This is in agreement with the results of previous studies<sup>7–9</sup> that have reported the stabilization of this phase in films epitaxially grown on STO substrates. The out-of-plane lattice parameter of the film has been determined from the

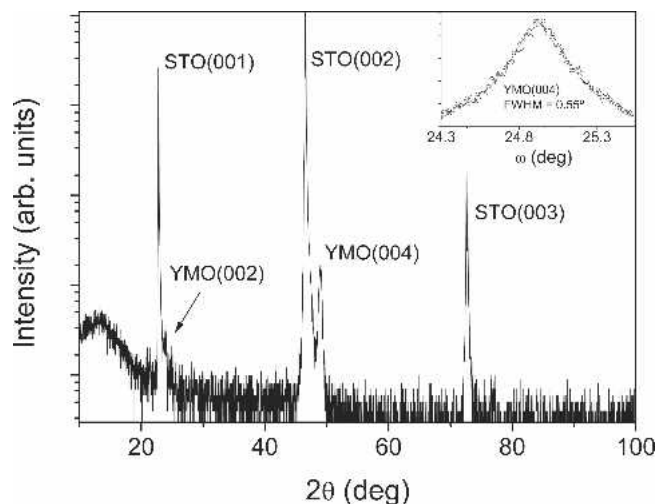


FIG. 1. XRD diffraction pattern of the YMO/NbSTO(001) sample. The reflections from the film correspond exclusively to the YMnO<sub>3</sub> orthorhombic phase with (001) out-of-plane texture. Inset:  $\omega$  scan around the YMO(004) reflection.

position of the YMO(004) peak, after a calibration by using the STO(002) reflection. The obtained value for the film ( $c_{\text{film}} = 7.43 \text{ \AA}$ ) indicates an expansion of the lattice parameter ( $c_{\text{bulk}} = 7.36 \text{ \AA}$ , with the strain being  $\epsilon_{[001]} = +0.95\%$ ). On the other hand, we show in the inset of Fig. 1 the rocking curve ( $\omega$  scan) of the YMO(004) reflection, which has a full width at half-maximum of  $0.55^\circ$ , whereas the instrumental resolution is  $0.02^\circ$  as determined by rocking curves on the STO(002) peak.

Although the rocking curve of this symmetrical reflection is only relatively narrow, the film is epitaxial, as evidenced by the pole figures. In Fig. 2(a), we have collected the poles from the YMO(111) and the STO(111) planes. As expected, there are four narrow {111} peaks,  $90^\circ$  apart, which arise from the substrate. In contrast, the four peaks corresponding to the (111) reflections from the YMO film are notably wide (around  $15^\circ$ ) along  $\phi$ . The four peaks are, as the substrate peaks, roughly  $\sim 90^\circ$

apart, and are rotated in-plane by  $45^\circ$  with respect to those of the STO(111) planes. We notice that due to the orthorhombic symmetry of YMO, two pairs of peaks were expected, with angular splitting  $\Delta\phi$  differing gradually from  $\Delta\phi = 90^\circ$  as the orthorhombicity ( $b/a$ ) increases. Therefore, a detailed analysis of the YMO(111) reflections of the pole figure in Fig. 2(a) is required. An intensity profile along  $\phi$  of one of the YMO(111) peaks of Fig. 2(a) is shown in Fig. 2(b). It becomes clear that, in fact, two peaks contribute to each spot, indicating that each reflection is doubled. Thus, there are eight peaks that correspond to a pair of crystal variants, with orthorhombic symmetry and  $90^\circ$  rotation in-plane. Taking into account the position of the STO(111) reflections, the epitaxial relationships of these two variants are:  $[100]\text{YMO}(001)/[110]\text{STO}(001)$ ; and  $[010]\text{YMO}(001)/[110]\text{STO}(001)$ . It has to be noted that if the film were fully relaxed with in-plane cell parameters identical to those of bulk YMO, the two peaks shown in Fig. 2(b) should be separated by  $6.06^\circ$ . However, they are separated by  $5.76^\circ$ , and this means that the film is not fully relaxed, but is partially strained. Similar films grown on undoped STO(001) substrates showed the same splitting in  $\phi$  and the same out-of-plane lattice parameter, and detailed characterization by means of reciprocal space maps allowed the determination of the in-plane lattice parameters. The in-plane cell parameters were found to be  $a = 5.26(1) \text{ \AA}$  and  $b = 5.80(1) \text{ \AA}$ ; this indicates that the film is fully relaxed along the  $[100]$  crystal direction but only partially strained along the  $[010]$  direction ( $\epsilon_{[010]} = -0.85\%$ ). Additional characterization of the twinning and a discussion of its impact on the relief of the elastic energy of the film will be reported elsewhere.<sup>14</sup> Notice that the Mn spins in the o-YMO lie along the partially strained  $[010]$  direction. Therefore, the interatomic Mn–O–Mn bonds in the YMO film are expected to vary with respect to the bulk bonds, possibly modifying the magnetic properties.

The temperature dependence of the magnetic moment of the YMO–NbSTO sample was measured, after zero-field cooling (ZFC) and field cooling (FC) procedure. The magnetic field was applied in-plane of the film. The open and closed symbols in Fig. 3(a) correspond to the FC and ZFC data, respectively, collected using a 1-kOe magnetic field. Inspection of the data shows that the ZFC–FC curves split apart at temperatures below  $\sim 45 \text{ K}$ , which we identify with the  $T_N$ ; the ZFC curve displays a broad maximum at  $T_{\text{max}} \sim 25 \text{ K}$  and decreases gradually at lower temperatures. In contrast, the FC curve keeps growing when the temperature further decreases. The measured magnetic moment contains the contribution from the YMO film added to that of the substrate. As the magnetic moment of the thin film, both in the paramagnetic and magnetically ordered state, is weak and comparable to that of the substrate (Nb–STO in the present

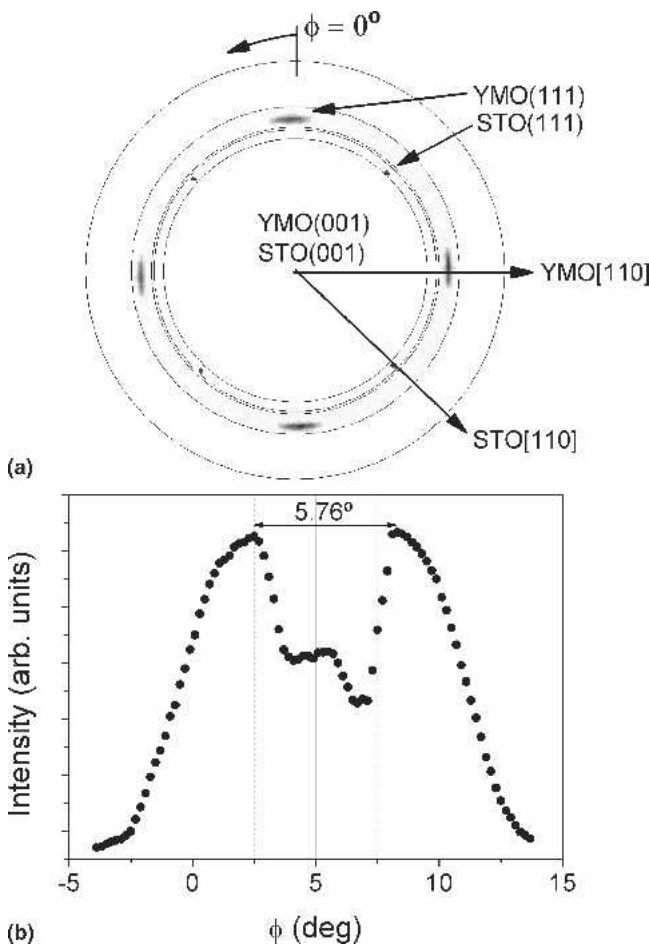


FIG. 2. (a) Plot collecting the XRD pole figure of the STO(111) and the YMO(111) reflections; different intensity scales are used for the substrate and film reflections. (b) Intensity profile along  $\phi$  corresponding to a YMO(111) reflection showing the double contribution in this reflection.

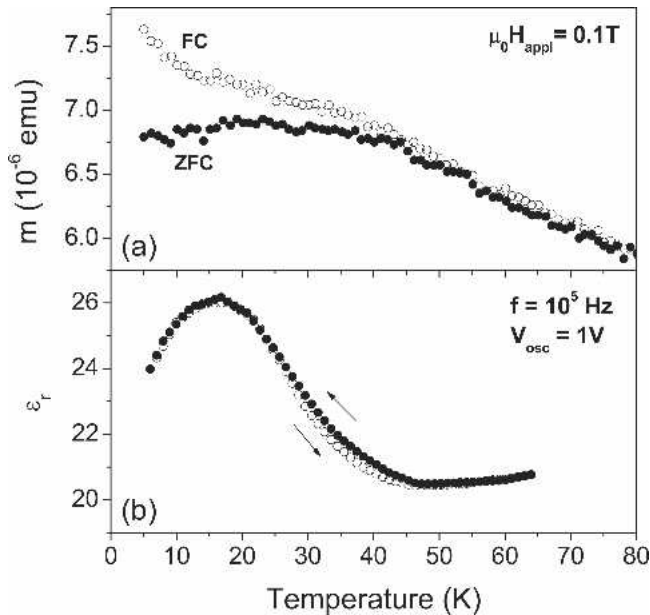


FIG. 3. (a) Temperature dependence of the magnetic moment of the YMO/NbSTO(001) sample measured at warming after ZFC (closed symbols) and FC (open symbols). (b) Relative permittivity of the o-YMO film evaluated from our measurements when cooling (closed symbols) and warming (open symbols) the sample.

case), the magnetization of the YMO film can not be determined with great accuracy. However, the cusp in the ZFC curve and the irreversibility in the magnetic response, which are manifested in the difference between the FC and ZFC curves, clearly show the occurrence of long-range magnetic order and are indicative for the existence of a ferromagnetic component in the response. Note that both features are absent in the magnetic response of the substrate, and thus the data in Fig. 3(a) represent genuine properties of o-YMO films.<sup>15</sup>

Before discussing the magnetic data, it is worth to recall that in these experiments the magnetic field is applied in-plane, and, thus, according to structural analysis, the field is parallel to the  $a$ - $b$  plane, which is the plane where, in bulk materials, the Mn magnetic moments are confined. Under these experimental conditions, the magnetization of an ideal AF material would display a kink at the  $T_N$  followed by some nonhysteretic magnetization reduction at lower temperature. The data in Fig. 3(a) do not follow these trends.

The absence of sharp features in the direct current (dc) magnetization curves at the  $T_N$  of o-YMnO<sub>3</sub> was noticed earlier, although its ultimate cause has not been definitely settled, and somehow contradictory results have been reported. In the dc magnetization data reported by Muñoz et al.,<sup>12</sup> only a subtle kink is visible at about 40 K. In contrast, earlier measurements by Wood et al.<sup>6</sup> and more recent data by Lorenz et al.<sup>10</sup> display a  $\lambda$ -like peak at  $T_N$ . The observation of hysteresis in ZFC–FC data is inter-

esting on its own. Thermal hysteresis of the magnetization is also visible in the data reported by Lorenz et al.<sup>10</sup> Muñoz et al.<sup>12</sup> also noticed that the alternating current magnetic susceptibility displays a maximum at around  $T = 11$  K, which they attributed to the freezing temperature associated with the partial spin-glass behavior of the sample, although no magnetic hysteresis was observed. It was argued that this spin-glass behavior could be originated by the presence of some Mn<sup>4+</sup> ions, resulting from tiny oxygen excess, and the subsequent magnetic disorder. On the other hand, non-stoichiometry-related defects could lead to the formation of Mn<sup>3+/4+</sup> states. In that case, double-exchange Mn<sup>3+/4+</sup>–Mn<sup>3+/4+</sup> ferromagnetic interactions can be introduced, thus leading to competing ferromagnetic–AF interactions or even ferromagnetic clusters that may behave as a superparamagnet or eventually a spin-glass-like material at low temperatures. The divergence of ZFC–FC curves is found both in spin-glass systems and in superparamagnetic systems; thus, this feature cannot be taken as a univocal hallmark of spin-glass behavior. We also noticed that hysteretic ZFC–FC data could also be expected if there is a magnetic canting that give rise to a long-range, ordered, weak ferromagnetism. The present experiments do not allow discrimination among these different scenarios. As already reported in the literature, linear susceptibility may not be sensitive enough to unravel the origin of magnetic hysteresis, but a higher-order harmonic susceptibility analysis is required.<sup>16,17</sup> Indeed, this is a crucial point that would require further experimental efforts.

Maybe of greater relevance here is that the strain induced by the substrate, and the resulting change of bond angles and distances, could modify some magnetic interactions, eventually reinforcing the competition between them. This is a very appealing possibility, and the fact that the ZFC–FC divergence is more pronounced in these o-YMnO<sub>3</sub> thin films than what had been reported earlier for bulk materials suggests that substrate-induced strain can play an important role. However, we can not neglect a possible contribution of stoichiometry-related defects to the appearance of the weak ferromagnetic character. Further experiments are required to discriminate among these effects.

Now, we address the dielectric measurements performed on the very same sample. Measurements of permittivity and magnetodielectric response in thin films are particularly challenging.<sup>18</sup> Therefore, we shall discuss in some detail the methodology used. Two samples, a bare NbSTO substrate and the o-YMO/NbSTO film/substrate, were mounted on a sample holder of the PPMS, and their impedance was measured using two dedicated wires.

Figure 4 shows the temperature dependence of the capacitance ( $C_s$ ) of a bare NbSTO substrate (open symbols) and ( $C_{sf}$ ) of the o-YMO/NbSTO films/substrate

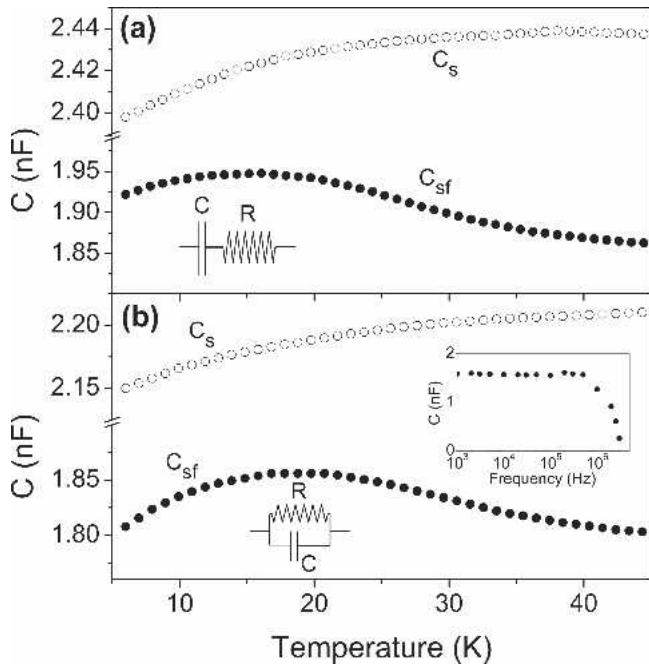


FIG. 4.  $C_s$  (open symbols) and  $C_{sf}$  (closed symbols) versus temperature, using for data collecting either (a) a series or (b) a parallel RC model. The inset in (b) shows the frequency dependence of  $C_{sf}$ .

sample (closed symbols). The complex impedance and conductance were measured using an excitation voltage of 1 V at 100 kHz; the measured values of impedance and conductance are about 500  $\Omega$  and 1.5 mS, respectively.  $C_s$  and  $C_{sf}$  were subsequently calculated by assuming two resistor–capacitor (RC) circuits: a series RC [Fig. 4(a)]; and parallel RC [Fig. 4(b)]. We note in Fig. 4 that both model circuits lead to very similar values for the capacitances. In addition, in the frequency range of 1 kHz to 1 MHz, the magnitude of the capacitances is constant [see inset in Fig. 4(b)]; therefore, we assume that the major contribution to the measured capacitance originates from the sample under study and that the data are free of spurious effects.

In Fig. 4, we observe that the contribution from the substrate and wiring ( $C_s$ ) monotonically decreases as the sample is cooled down. The temperature dependence of the capacitance of the o-YMO/NbSTO films/substrate sample  $C_{sf}$  is very different: it exhibits a maximum at  $T \approx 16$  K. It is remarkable that this  $C_{sf}$  peak starts to develop at the same temperature ( $\sim 45$  K) at which the divergence of the ZFC–FC magnetization curves is observed, as shown in Fig. 3(a). To extract the relative permittivity ( $\epsilon_r$ ) of the o-YMO film, we proceeded as follows. We modeled the measured capacity  $C_{sf}$  of the sample under study (YMO–NbSTO) with a simple circuit: a series combination of capacitors,  $C_{sf}^{-1} = C_s^{-1} + C_f^{-1}$ , where the term  $C_s$  includes all parasitic contributions due to the substrate and wiring, and  $C_f$  is the capacitance of the o-YMO film. From the experimental

values of  $C_s$  and  $C_{sf}$  (Fig. 4), the  $C_f$  can be evaluated. As illustrated by the data in Figs. 4(a) and 4(b), the values of capacitance do not differ significantly if a series or a parallel RC measuring circuit is assumed; therefore, in the following series  $C_s$  and  $C_{sf}$  values [Fig. 4(a)] will be used. The permittivity of the o-YMO film is subsequently calculated considering an ideal capacitor with parallel electrodes,  $C_f = \epsilon \times A/t$ , where  $A$  and  $t$  ( $A \approx 8$  mm<sup>2</sup> and  $t \approx 150$  nm) stand for the area of the graphite contacts and the thickness of the o-YMO film, respectively. The temperature dependence of the relative dielectric constant ( $\epsilon_r$ ) obtained from measurements increasing or decreasing  $T$  is shown in Fig. 3(b) (open and closed circles, respectively).

We first note that the magnitude of  $\epsilon_r \approx 20$ –25 is very similar to that reported by Lorenz et al.<sup>10</sup> for polycrystalline samples. Next, it is clear that when cooling down across the magnetic transition ( $T_N \sim 45$  K),  $\epsilon_r(T)$  starts growing and reaches a maximum (26% larger value) at  $T \approx 16$  K. Notice that the temperature dependence of the permittivity mimics the ZFC magnetization curve. Thus, the observed behavior is just the counterpart of the magnetodielectric effect observed by Lorenz et al.<sup>10</sup> in bulk o-YMnO<sub>3</sub>. The subtle thermal hysteresis that is visible in Fig. 3(b) is much smaller than that observed in the polycrystalline samples. Magnetocapacitance could be also visible when applying an external magnetic field. We measured the capacitance of the films under a magnetic field of 9 T that was applied perpendicular to the film surface. Unfortunately, any change in capacitance, if it exists, is below the noise level. We recall that the magnetocapacitance measurements on polycrystalline YMO samples, reported by Lorenz et al.,<sup>10</sup> gave changes only for  $\Delta\epsilon/\epsilon$  of  $\sim 1.5\%$  at 7 T. The ultimate reason for the observed weak effect of the external magnetic field on the dielectric response, particularly when compared to the huge peak that  $\epsilon_r$  displays when magnetic order sets in, is unknown. A detailed microscopic understanding of the magnetoelectric coupling in orthorhombic manganites, which is not yet available, would be required. We noticed, however, that the applied magnetic field is several orders of magnitude smaller than the internal molecular Weiss field in the magnetic material; thus, one could anticipate weak effects in magnetic fields under 9 T.

#### IV. SUMMARY

In summary, we have shown that epitaxial orthorhombic YMnO<sub>3</sub> films grown on Nb:STO(001) substrates display a remarkable change in permittivity when the AF order sets in. This observation mimics previous results that have been reported for bulk materials. Moreover, we have observed a genuine ZFC–FC hysteresis in the magnetization curves, which has not been reported in bulk

materials. We have proposed that this behavior could be attributed to the appearance of a ferromagnetic component that is associated with the modification of the magnetic interactions in thin films, due either to the strain-induced modification of the magnetic interactions or to the presence of non-stoichiometry-related defects. It follows that the appropriate selection of growth conditions and substrates could allow the tuning of the magnetic response of YMnO<sub>3</sub>.

## ACKNOWLEDGMENTS

Financial support was given by the Ministerio de Educación y Ciencia (MEC) of the Spanish Government (projects NAN2004-9094-C03 and MAT2005-5656-C04) and by the European Union [project MaCoMuFi (FP6-03321)] are acknowledged.

## REFERENCES

1. E.F. Bertaut, F. Forrat, and P. Fang: A new class of ferroelectrics: Rare earth and yttrium manganites. *Compt. Rend.* **256**, 1958 (1963).
2. R. Pauthenet and C. Veyret: Magnetostatic properties of rare earth manganites. *J. Phys. E: Sci. Instrum.* **31**, 236 (1965).
3. T. Kimura, T. Goto, H. Shintani, K. Ishizaka, T. Arima, and Y. Tokura: Magnetic control of ferroelectric polarization. *Nature* **426**, 55 (2003).
4. B.B. Van Aken, T.T.M. Palstra, A. Filippetti, and N.A. Spalding: The origin of ferroelectricity in magnetoelectric YMnO<sub>3</sub>. *Nat. Mater.* **3**, 164 (2004).
5. M. Mostovoy: Ferroelectricity in spiral magnets. *Phys. Rev. Lett.* **96**, 067601 (2006).
6. V.E. Wood, A.E. Austin, and E.W. Collings: Magnetic properties of heavy rare earth orthomanganites. *J. Phys. Chem. Solids* **34**, 859 (1973).
7. P.A. Salvador, T.D. Doan, B. Mercey, and B. Raveau: Stabilization of YMnO<sub>3</sub> in a perovskite structure as a thin film. *Chem. Mater.* **10**, 2592 (1998).
8. O. Yu Gorbenko, S.V. Samoilenkov, I.E. Graboy, and A.R. Kaul: Epitaxial stabilization of oxides in thin films. *Chem. Mater.* **14**, 4026 (2002).
9. X. Martí, F. Sánchez, J. Fontcuberta, M.V. García-Cuenca, C. Ferrater, and M. Varela: Exchange bias between magnetoelectric YMnO<sub>3</sub> and ferromagnetic SrRuO<sub>3</sub> epitaxial films. *J. Appl. Phys.* **99**, 302 (2006).
10. B. Lorenz, Y.Q. Wang, Y.Y. Sun, and W. Chu: Large magneto-dielectric effects in orthorhombic HoMnO<sub>3</sub> and YMnO<sub>3</sub>. *Phys. Rev. B* **70**, 212412 (2004).
11. S. Quezel, J. Rossat-Mignod, and E.F. Bertaut: Magnetic structure of rare earth orthomanganites: 1. YMnO<sub>3</sub>. *Solid State Commun.* **14**, 941 (1974).
12. A. Muñoz, J.A. Alonso, M.T. Casais, M.J. Martínez-Lope, J.L. Martínez, and M.T. Fernández-Díaz: The magnetic structure of YMnO<sub>3</sub> perovskite revisited. *J. Phys.: Condens. Matter* **14**, 3285 (2002).
13. H.W. Brinks, J. Rodríguez-Carvajal, H. Fjellvag, A. Kjekshus, and B.C. Hauback: Crystal and magnetic structure of orthorhombic HoMnO<sub>3</sub>. *Phys. Rev. B* **63**, 094411 (2001).
14. X. Martí, F. Sánchez, V. Skumryev, V. Laukhin, M.V. García-Cuenca, C. Ferrater, M. Varela, and J. Fontcuberta: Crystal texture selection in epitaxies of orthorhombic antiferromagnetic YMnO<sub>3</sub> films. *Thin Solid Films*, submitted for publication.
15. V. Skumryev, X. Martí, F. Sánchez, V. Laukhin, and J. Fontcuberta: in preparation.
16. S. Nair and B. Banerjee: Probing a ferromagnetic critical regime using nonlinear susceptibility. *Phys. Rev. B: Condens. Matter* **68**, 094408 (2003).
17. G. Sinha and A.K. Majumdar: Linear and non-linear AC susceptibilities in different magnetic phases of Fe-rich gamma-FeNiCr alloys. *J. Magn. Magn. Mater.* **185**, 18 (1998).
18. G. Catalan: Magnetocapacitance without magnetoelectric coupling. *Appl. Phys. Lett.* **88**, 102902 (2006).